J Membrane Biol (2009) 232:1–13
DOI 10.1007/s00232-009-9206-0

ORIGINAL ARTICLES

Cell Migration in BeWo Cells and the Role of Epithelial Sodium Channels

Silvana M. del Mónaco · Gabriela I. Marino · Yanina A. Assef · Alicia E. Damiano · Basilio A. Kotsias

Received: 8 June 2009 / Accepted: 23 September 2009 / Published online: 13 November 2009

Abstract Cell migration/proliferation processes associated with wound healing were measured in BeWo cells at 6 h, when mitosis is still scarce. Cells were cultured in medium with 1% fetal bovine serum to minimize proliferation. BeWo cell migration covered 20.6 ± 7.0%, 38.0 ± 5.4%, 16.6 ± 4.8% and 13.7 ± 3.6% of the wound when cultivated under control, aldosterone (100 nM, 12 h), aldosterone plus amiloride (10 μM) and amiloride treatments, respectively. When BeWo cells were treated with aldosterone, there was an increase in wound healing ($P < 0.05$), which was prevented by adding the ENaC blocker amiloride ($P < 0.05$, $n = 16$). Immunocytochemistry studies showed that the three ENaC subunits showed greater expression at the leading edge of the wound 3 h after injury, supporting the notion that these proteins participate in a postinjury signal. Antisense oligonucleotides directed against the α-ENaC subunit decreased the migratory response of the cells compared to the sense treated cells or the cells without oligonucleotides ($P < 0.001$, $n = 16$): 30.2 ± 3.7%, 17.6 ± 1.3%, 27.5 ± 1.5% and 20.2 ± 1.5% reinvasion of the wound with aldosterone, aldosterone plus antisense, aldosterone plus sense treatments and control conditions, respectively. Aldosterone and amiloride influence wound healing in BeWo cells, probably by their effects upon ENaCs, transmitting a signal to the cell cytoplasm for the release of several agents that promote cell migration.

Keywords BeWo cell · Wound healing · ENaC · Migration

S. M. del Mónaco · G. I. Marino · Y. A. Assef · B. A. Kotsias (✉)
Laboratorio de Canales Iónicos, Instituto de Investigaciones Médicas A. Lanari, Universidad de Buenos Aires, C. de Malvinas 3150, 1427 Buenos Aires, Argentina
e-mail: kotsias@retina.ar

A. E. Damiano
Laboratorio de Biología de la Reproducción, Cátedra de Biología Celular, Facultad de Farmacia y Bioquímica, Universidad de Buenos Aires, Buenos Aires, Argentina

Introduction

The epithelial sodium channel (ENaC) mediates entry of Na^+ from the luminal fluid into the cells in many reabsorbing epithelia (Alvarez de la Rosa et al. 2002). The channel is composed of three homologous subunits α, β and γ; it is blocked by the diuretic amiloride (Kellenberger and Schild 2002), and it is sensitive to aldosterone, vasopressin, prostaglandin, catecholamine, estrogen and progesterone stimuli (Gambling et al. 2004; Snyder 2005; Butterworth et al. 2009) as well as to the cytosolic pH (Reddy et al. 2008). Investigations on ENaCs are difficult because of the low abundance of channels in hormone-unstimulated tissues. In this regard, aldosterone modulation produces an increase in trafficking and apical membrane expression (May et al. 1997; Verrey et al. 2008; Alvarez de la Rosa et al. 2002; Malik et al. 2006; McEneaney et al. 2008) and an increase in open probability due to channel proteolysis (Kemendy et al. 1992; Hughey et al. 2003; Caldwell et al. 2004; Wakida et al. 2006; Harris et al. 2007; Diakov et al. 2008) and methylation (Edinger et al. 2006; McEneaney et al. 2008).

Na^+ currents mediated by ENaCs are involved in cell migration, which is well documented in epithelial and

vascular cells (Chifflet et al. 2005; Grifoni et al. 2006) and in the proliferation of tumor cells (Sparks et al. 1983; Vila-Carriles et al. 2006). Cell migration has an important role in many physiological processes, such as implantation and embryogenesis, immunity and inflammation, tissue regeneration, angiogenesis and metastasis (Schwab et al. 2005). Cell motion mechanisms are related to cytoskeletal reorganization, where cortical actin filaments are involved in the generation of locomotive structures and in the interaction with other signaling and structural proteins (Mitchison and Cramer 1996). Ion channels and transporters actively participate in this process, being regulated by cytoskeletal components and cell volume (Mills and Mandel 1994; Schwab et al. 2005). Thus, there is an interaction between the ENaC and the membrane cytoskeleton (Smith et al. 1991; Cantiello et al. 1991; Rotin et al. 1994; Berdiev et al. 1996; Golestaneh et al. 2001; Copeland et al. 2001; Mazzochi et al. 2006). In addition, the channel belongs to a protein family which includes mechanoreceptors and it has been suggested that it possesses a mechanical signal-translating function (Carattino et al. 2004; Drummond et al. 2004, 2006; Wei et al. 2007).

Two points were important for the development of this work. First, BeWo cells, a human hormone-synthesizing trophoblastic cell line, express the three subunits of the ENaC and present ENaC-like currents when stimulated with aldosterone (del Mónaco et al. 2006, 2008b). Second, there is a possible relation between cell migration defects and preeclampsia. Preeclampsia is a high-incidence heterogeneous multisystem disorder of unknown etiology that may cause fetal injury and growth retardation as well as endothelial cell activation/dysfunction in a susceptible mother. One of the proposed mechanisms could be impaired trophoblast invasiveness and defects in spiral arterial remodeling, as observed in some cases of preeclampsia (Sibai et al. 2005; Myatt 2006; Huppertz 2008). In this work we tested the hypothesis that the ENaC is required for the migration of BeWo cells. We performed a series of experiments measuring cell migration/proliferation processes associated with wound healing in BeWo cells. The results show that aldosterone and amiloride treatments influence wound healing in BeWo cells, probably by their effects upon ENaCs. We observed that cellular migration, and not cellular proliferation, is the main factor for this phenomenon and that ENaC density is increased in the wound border. Reducing the expression of α-ENaC by antisense oligonucleotides produced a significant inhibition in wound healing and in current stimulation. ENaC expression in human placenta was assessed to validate the physiological relevance of these data and to extrapolate them to actual human tissue. Preliminary results from this work were presented elsewhere (del Mónaco et al. 2008a).

Methods

Cell Culture

The BeWo cell line was obtained from the American Type Culture Collection (Rockville, MD). Cells were cultured in Ham's F12 medium (GIBCO BRL, Life Technologies, Grand Island, NY) supplemented with 10% fetal bovine serum (FBS; Natocor Biotechnology, Córdoba, Argentina), 2 mM L-glutamine (Sigma, St. Louis, MO), 100 U/ml penicillin and 100 mg/ml streptomycin. Cells were harvested once a week with 0.25% trypsin–EDTA (GIBCO BRL, Life Technologies) and incubated at 37°C in humid air with 5% CO_2. Aldosterone (100 nM, Sigma) was added to the culture medium when needed.

Wound-Healing Assay

Cell concentration was adjusted to 2×10^5 cells/cm^2, and cells were seeded onto 24-well plates in Ham's F12 medium containing 10% FBS, until achieving a confluent cell layer. Hormone-treated cells were incubated overnight with 100 nM aldosterone. Monolayers were manually scraped with a 200-μl pipette tip and washed with medium without serum to remove nonadherent cells. Then, Ham's F12 1% FBS was added to attenuate cellular proliferation without impairing cell survival, with four different treatments: (1) a control group with the drug vehicles, (2) 100 nM aldosterone, (3) 100 nM aldosterone plus 10 μM amiloride and (4) 10 μM amiloride. Cells were cultured in an incubator at 37°C in humid air with constant 5% CO_2. Wound scraping was considered time 0, and images of the wounded area were taken under the microscope at different times after the injury (0, 6, 12, 24, 36, 48 and 60 h), photographing the same area at each time interval. Healing was quantified using ImageJ 1.39 software (Image Processing and Analysis in Java, NIH, Bethesda, MD). A mark was made in each well to measure the same spot at every time. Images were observed at the same magnification. A straight line was traced in the images, crossing the wound through the denuded area, and the number of pixels was determined using the measuring command of the program. The straight line length expressed in pixels was considered to represent the width of the wound at each time analyzed. Results were expressed as reinvasion percentage of the wound compared to time 0 (mean ± standard deviation). Experiments were repeated 16 times with four different cell passages.

Antisense and Sense Oligonucleotides to α-ENaC

Oligonucleotides either complementary (for antisense) or identical (for sense) to the α-ENaC start sequence including

the initiation codon ATG were synthesized as the phosphothiorate oligonucleotides. The sequences were as follows: α-sense 5′-TACCAGGTCTCATGGA-3′ and α-antisense 5′-TTCCCCTCCATGAGA-3′ (Ma et al. 2004). Cells were pretreated with 1% FBS medium containing either 10 μm antisense or sense oligonucleotides for 24 h and 100 nM aldosterone for the last 12 h. Control treatments were carried out without aldosterone stimulation, and a treatment with aldosterone but without oligonucleotides was also performed. Oligonucleotides were repeatedly added into the culture medium every 6 h to ensure their presence in the adequate concentration. When the monolayer was scraped, oligonucleotide doses were mixed with the appropriate amount of LipofectAMINE™ Reagent (GIBCO BRL, Life Technologies) to favor delivery into the cells. Wound-healing assays with the pretreated cells were performed as previously described. We used this approach because Forbes et al. (2009) demonstrated that siRNAs have very little effect on decreasing protein expression in BeWo cells.

Whole-Cell Recordings

Electrophysiological studies were carried out as described previously (del Mónaco et al. 2008b). Briefly, cells were grown on glass coverslips, washed with bath solution and transferred into the patch recording chamber mounted on the stage of an Olympus (Tokyo, Japan) inverted microscope. Electrical activity was recorded in the whole-cell configuration with standard patch-clamp technology by means of an amplifier with a 1 GX feedback resistor (List L/M-EPC7; List Medical Electronics, Darmstadt, Germany). Electrical signals were analyzed using Pclamp v.8 software (Axon Instruments, Union City, CA). Whole-cell configuration was established with polished standard glass micropipettes (World Precision Instruments, Sarasota, FL) with a tip resistance of 2–4 MΩ when filled with pipette solution. The series resistance (Rs) was compensated for using the analog circuit of the amplifier. The protocol consisted of pulses from +40 to −140 mV in steps of 20 mV, from a holding potential of 0 mV and with a 10-ms interval between each pulse. Current–voltage (I–V) plots were obtained from currents measured in a stationary state and expressed as current densities (current per unit cell capacitance). The capacitance of the cells (Cm) was measured by applying 100 ms, 10 mV, depolarizing pulses from a holding potential of 0 mV. The currents were fitted to an exponential function and the time constant (s) was measured; thus, Cm = s/Rs. All experiments were done at room temperature (20–24°C).

Pipette solution (intracellular) contained (in mM) 102 K-gluconate, 6 KCl, 4 $MgCl_2$, 3 EGTA, 10 HEPES and 50 mM sucrose (pH 7.4). Bath solution contained (in mM) 105 NaCl, 4 KCl, 3 $CaCl_2$, 3 $MgCl_2$, 10 HEPES and 40 sucrose (pH 7.4).

Cells were cultivated with 10 μM antisense or sense oligonucleotides for 24 h and 100 nM aldosterone for the last 12 h. Oligonucleotides were repeatedly added into the culture medium every 6 h to ensure their presence in adequate concentration. During whole-cell experiments, cells were exposed to 100 μM 8Br-cAMP for 30 min and to 10 μM amiloride (Sigma) (in the presence of cAMP) until maximal blockage was achieved. Drugs were diluted in distilled water and DMSO and added directly to the chamber containing the cells in solution. The DMSO final concentration per se did not affect ion channel activity (data not shown).

BeWo Cell Immunoblotting

BeWo cell layers were washed with phosphate-buffered saline buffer (PBS; GIBCO BRL, Life Technologies) and scraped into ice-cold PBS buffer with 0.01× protease inhibitor cocktail (PIC) and 0.2 mM phenylmethanesulfonyl fluoride (Sigma). Cells were then centrifuged and resuspended in lysis buffer (0.3 M NaCl, 25 mM HEPES, 1.5 mM $MgCl_2$, 0.2 mM EGTA, 1% Triton X-100 [pH 7.4]) with protease inhibitors. The homogenate was spun for 5 min at 10,000 rpm (4°C), and the supernatant was collected and stored at −20°C. Total protein amount in each sample was assessed using the Bradford protein assay (Bradford reagent, Sigma).

For immunoblot studies, 75 μg of BeWo proteins were dissolved in loading buffer (4% sodium dodecyl sulfate, 0.125 M Tris–HCl [pH 6.8], 0.2 M dithiothreitol, 0.02% bromophenol blue, 20% glycerol) and heated to 100°C for 2 min. Samples were resolved on 8% polyacrylamide gel and electrotransferred onto nitrocellulose membranes (Hybond ECL; Amersham Pharmacia Biotech, Little Chalfont, UK). Membranes were blocked for 1 h at room temperature with 2% (w/v) defatted milk in Tris-buffered saline-Tween 0.1% (T-TBS) and incubated overnight with anti-ENaC antibodies in T-TBS buffer supplemented with 0.5% (w/v) bovine serum albumin (BSA, Sigma). To detect the α-ENaC subunit we used a rabbit polyclonal antibody directed against amino acid residues 131–225 of human α-ENaC at a dilution of 1:1,000, and to detect α-tubulin we used a mouse polyclonal antibody at a dilution of 1:5,000 (Santa Cruz Biotechnology, Santa Cruz, CA). Membranes were washed with T-TBS and then incubated for 1 h at room temperature with goat anti-rabbit or anti-mouse secondary antibodies conjugated to peroxidase (1:5,000) (Vector Lab, Burlingame, CA). Filters were washed and positive reactivity was detected using the ECL Western Blotting Analysis System (Amersham Biosciences, Buenos Aires, Argentina). The chemiluminescence reaction was

visualized on AGFA Medical X-Ray films (Agfa-Gevaert, Buenos Aires, Argentina).

MTT Assay

Cell proliferation was assessed using the 3-(4,5-dimethylthiazol-2-yl)-2,5-diphenyl tetrazolium bromide (MTT, Sigma) assay. BeWo cells were incubated in 96-well culture plates in Ham's F12 medium with 10% FBS and grown until achieving a confluent layer. Cells were tested for the same treatments described above for 2 h. Then, 20 µl of MTT (5 mg/ml in PBS) were added to each well and incubated for 4 h at 37°C. The MTT formazan precipitate was dissolved in 100 µl of DMSO. Optical density was measured at 570 nm (OD_{570nm}) on an ELISA plate reader (R&D Systems, Minneapolis, MN), and cell proliferation for each treatment was calculated as a percentage of control (treated cultures OD_{570nm}/control cultures $OD_{570nm} \times 100$) and expressed as mean ± standard deviation. Experiments were repeated 21 times with four different cell passages.

Immunocytochemistry

BeWo cells were grown on untreated glass coverslips and cultured with Ham's F12 medium until optimal cell concentration. Culture medium was supplemented with 100 nM aldosterone for 12 h, and wounds were made as in the wound-healing experiments. After washing in culture medium, cells were fixed with a solution containing 3.7% formaldehyde and 0.12 M sucrose in 0.05 M PBS for 10 min at room temperature, followed by cell permeabilization in 0.2% Triton X-100 for 15 min. Blocking was made with 3% BSA in PBS buffer for 1 h at room temperature. Samples were incubated overnight with rabbit polyclonal antibodies directed against amino acid residues 131–225 of human α-ENaC and residues 411–520 of human γ-ENaC at a dilution of 1:100 and a mouse monoclonal antibody directed against amino acid residues 271–460 of human β-ENaC at a dilution of 1:100 (Santa Cruz Biotechnology). Cells were then washed with PBS and incubated for 1 h with anti-rabbit or anti-mouse fluorescein isothiocyanate (FITC)–conjugated secondary antibodies (Jackson Immunoresearch Laboratories, Tuker, GA). After washing the samples with PBS, they were mounted over glass plates in PBS/glycerol 1:1 solution. Samples were visualized with a fluorescence microscope, and digital images were taken with a digital camera coupled to the microscope. Images were analyzed with ImageJ 1.39 software. Experiments were performed at least two times, and a control study was performed, incubating the samples without primary antibody.

Tissue Collection

This study was approved by the local ethics committee of the Hospital Nacional Dr. Prof. Alejandro Posadas (Buenos Aires, Argentina), and written consent was obtained from patients before the collection of samples.

Human normal-term placentas of 37–42 weeks' gestational age were obtained immediately after spontaneous vaginal delivery or by cesarean section. Pregnant patients had maternal blood pressures ≤110/70 mm Hg, no proteinuria and no other complications. Maternal age had a range of 20–30 years.

Tissue was processed immediately in RNase-free conditions, to prevent RNA breakdown.

RT-PCR

Several cotyledons from term placentas were removed from underlying fibrous elements and rinsed thoroughly in 0.9% NaCl at 4°C. Soft villous material from the maternal surface enriched in syncytiotrophoblast was cut away from connective tissue and vessels until approximately 1 g were collected. The tissue was rinsed again in order to remove blood cells and then homogenized for 30 s on ice using a blender (Ultra-Turrax T25; IKA, Wilmington, NC) at maximum speed. Total RNA was isolated using the SV Total RNA isolation system (Promega, Madison, WI). Reverse transcription was performed using Moloney murine leukemia virus reverse transcriptase for 60 min at 42°C (Promega). The mixture also contained 5 µg of total RNA, oligo(dT)15 primers and 400 µM of each deoxyribonucleotide triphosphate (dNTP) (final volume 20 µl). PCR (50 cycles) was performed at 94°C for 60 s, 58°C for 60 s and 72°C for 60 s, followed by a final extension of 6 min at 72°C. The reaction was carried out using 5 µM of specifically designed oligonucleotide primers (Table 1). PCRs with actin primers were performed to test cDNA integrity. The control for the presence of genomic DNA was achieved because the primers for the α-subunit were designed to span introns between exons 5 and 6 and between exons 6 and 7. The expected size for the subunit using genomic DNA would be 1,023 bp, instead of the 257-bp fragment expected for a cDNA template (Bubien et al. 2001). PCR products were detected with ethidium bromide-stained 2% agarose gels in TBE buffer.

Cloning and Sequencing

The PCR product of placental α-ENaC was purified by means of electroelution. The product was inserted in the PGEMT-Easy vector (Promega), and Escherichia coli JM109 cells were transformed. The amplified plasmid was purified using a commercial kit (Wizard Plus SV Minipreps, Promega) and

Table 1 Designed oligonucleotide primers

Protein	Sequence	Fragment size (bp)
α-ENaC	Sense: 5′-GAA CAA CTC CAA CCT CTG GAT GTC-3′	257
	Antisense: 5′-TCT TGG TGC AGT CGC CAT AAT C-3′	
β-ENaC	Sense: 5′-TGC TGT GCC TCA TCG AGT TTG-3′	277
	Antisense: 5′-TGC AGA CGC AGG GAG TCA TAG TTG-3′	
γ-ENaC	Sense: 5′-TCA AGA AGA ATC TGC CCG TGA C-3′	237
	Antisense: 5′-GGA AGT GGA CTT TGA TGG AAA CTG-3′	
β-actin	Sense: 5′-CGG AAC CGC TCA TTG CC-3′	289
	Antisense: 5′-AAC CAC ACT GTG CCC ATC TA-3′	

sequenced in the Molecular Biology Laboratory (ArgenINTA Foundation, Castelar, Argentina).

Immunohistochemistry

Human villous tissues from normal-term placentas were cut into small pieces, fixed overnight in 10% formaldehyde–0.1 M sodium phosphate buffer (pH 7.4), dehydrated and embedded in paraffin. Paraffin sections (4–5 μm) were cut and mounted on 2% silanized slides, dried and deparaffinized in xylene (4 × 5 min), followed by short washes in 100 and 96% ethanol and distilled water. To enhance the immunoreactivity of proteins, slides were placed in diluted target retrieval solution 10× (Retrievit™-10 Target Retrieval Solution; BioGenex, San Ramon, CA), pH 10, and heated in a microwave for 20 min. Then, they were washed three times in PBS 1× (pH 7.4) for 3 min. All subsequent steps were carried out in a humidified chamber. Nonspecific binding sites were blocked by incubation at room temperature in blocking solution (PBS supplemented with 3% BSA) for 1 h. Sections were incubated overnight with the primary antibodies described above at a dilution of 1:100 and then washed with PBS 1×. Immunofluorescence was performed using anti-rabbit-FITC for detection of α- and γ-ENaC subunits and anti-mouse-FITC for β-ENaC (Jackson Immunoresearch Laboratories) at a dilution of 1:2,500 for 1 h at temperature room in all cases. Slides were mounted in PBS/glycerol 1:1 solution and analyzed on a fluorescence microscope (Axiostar plus HAL 100; Carl Zeiss, Oberkochen, Germany). Photographs were taken using a digital camera coupled to the microscope and analyzed with the software described above. Control samples were performed by omitting the primary antibody, and an additional control for α- and γ-ENaCs was carried out, incubating samples with total rabbit IgG (Santa Cruz Biotechnology).

Statistical Analysis

Data were expressed as mean values ± sd (n = number of cells analyzed). Statistical analysis was performed using ANOVA for multiple data comparison, followed by a post hoc test (Tukey or Dunnet test, when appropriate). Differences were considered statistically significant at $P < 0.05$.

Results

Aldosterone Influence in Wound Healing

A section of the cell layer was removed with the tip of a micropipette. This action left a clear space on the plastic for the cells to fill, and the wound border served as a migratory start line. This cleared space was subsequently visualized under the microscope and photographed to assess the ability of the cells to migrate and fill the wounded area.

Figure 1 shows examples of the wounded monolayers at 0, 6 and 60 h for the different treatments tested: (1) cells without stimulation, (2) cells stimulated with 100 nm aldosterone (12 h), (3) cells stimulated with 100 nm aldosterone and 10 μM amiloride and (4) cells treated with 10 μM amiloride.

As shown by Grifoni et al. (2006), cellular proliferation could mask the contribution of cell migration to wound healing. Thus, we tested wound healing at 6 h, when mitosis is still scarce, and used culture medium with 1% FBS, to minimize proliferation. The average values obtained at 6 h from 16 experiments are depicted in Fig. 2a (left). BeWo cells migrated covering 20.6 ± 7.0%, 38.0 ± 5.4%, 16.6 ± 4.8% and 13.7 ± 3.6% of the wound when cultivated under control, aldosterone, aldosterone plus amiloride and amiloride treatments, respectively. Only when cells were treated with aldosterone was there a significant increase in wound healing ($P < 0.05$), an effect that could be prevented by adding to the cells the ENaC blocker amiloride, alone or in combination with aldosterone ($P < 0.05$, $n = 16$). Cells treated with both stimuli did not show a difference from control samples, indicating that the blocker could inhibit the aldosterone-mediated

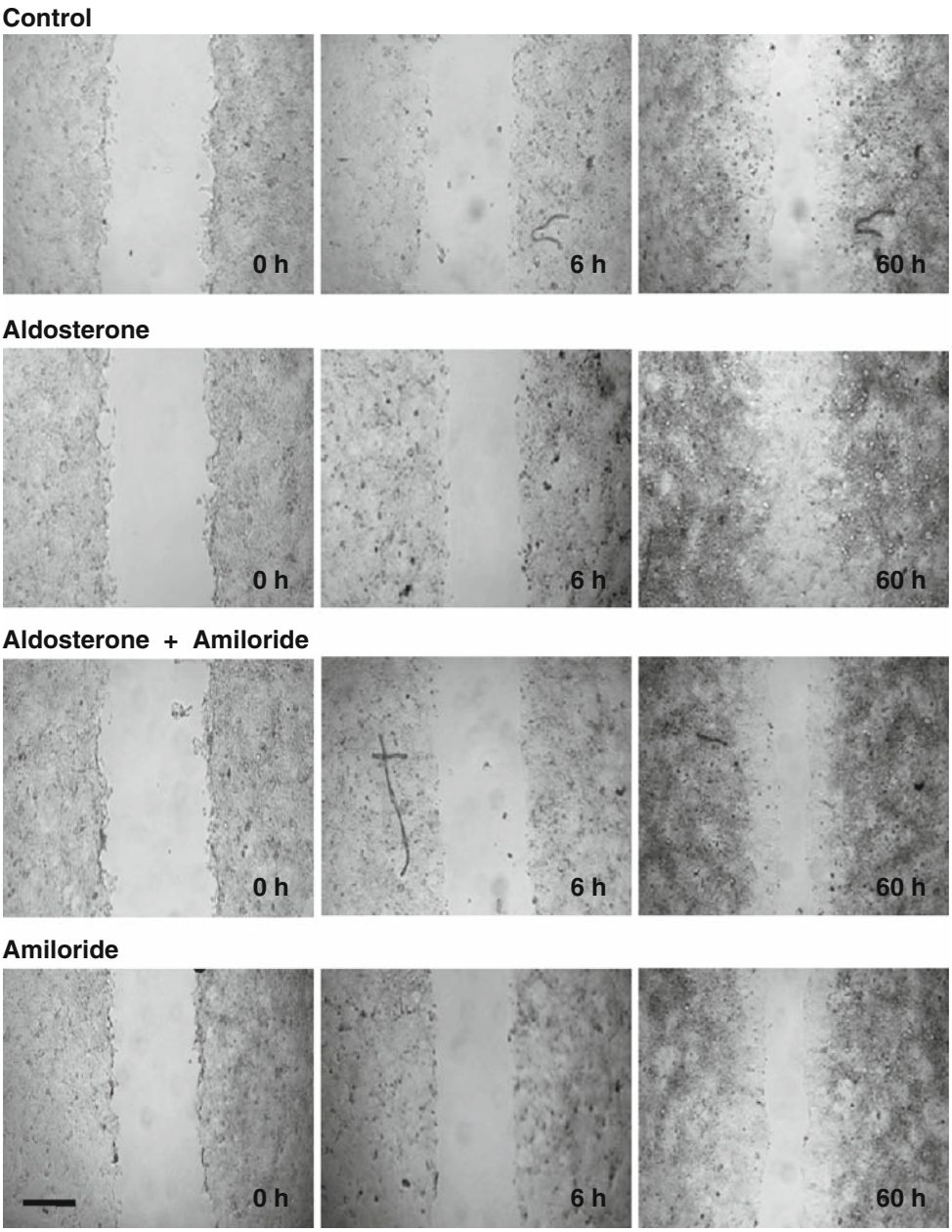

Fig. 1 Wound healing assay in BeWo cells. Images of BeWo epithelial sheets cultured under different treatments: (1) control conditions, (2) aldosterone 100 nM, (3) aldosterone 100 nM and amiloride 10 μM, (4) amiloride 10 μM. Pictures were taken when the sheets were wounded by scratching (time 0), 6 and 60 h later. In every picture the distance between each wound edge was estimated and results were expressed as percentage of reinvasion of the wound compared to time 0, to evaluate cell migration. The bar represents 200 μm

stimulation of ENaC activity. To confirm that cellular proliferation did not influence the wound-healing result, we measured cell proliferation with the MTT assay, following the same treatments (Fig. 2a, right). When BeWo cells were kept in 1% serum concentration, no changes in cell proliferation were seen in the 6 h culture in any treatment ($P > 0.05$). Nontreated cells were considered as 100% MTT reduction, and then 105.2 ± 6.5%, 110.8 ± 9.0% and 94.4 ± 5.4% MTT reductions were observed for the aldosterone, aldosterone plus amiloride and amiloride treatments, respectively ($P > 0.05$, $n = 21$). A noteworthy fact is that the aldosterone-treated cells could close a larger portion of the wound in the wound-healing assay without presenting an elevated proliferation compared with the control treatment. This would indicate that the healing process observed is mainly due to cell migration under our experimental conditions. Figure 2b shows the wound-healing time course under the different pharmacological conditions tested. Healing was calculated from the wound width at each time span (0, 6, 12, 24, 36, 48 and 60 h). The curves show similar results to those depicted in Fig. 2a (left). Clearly, aldosterone-treated cells showed greater healing behavior than the rest of the treatments, almost closing the wound at 60 h ($P < 0.01$, $n = 16$; 63.5 ± 14.6%, 94.3 ± 4.9%, 65.6 ± 11.6% and 58.0 ± 7.3% reinvasion of the wound with control, aldosterone, aldosterone plus amiloride and amiloride treatments, respectively). The MTT assay performed at 60 h showed that

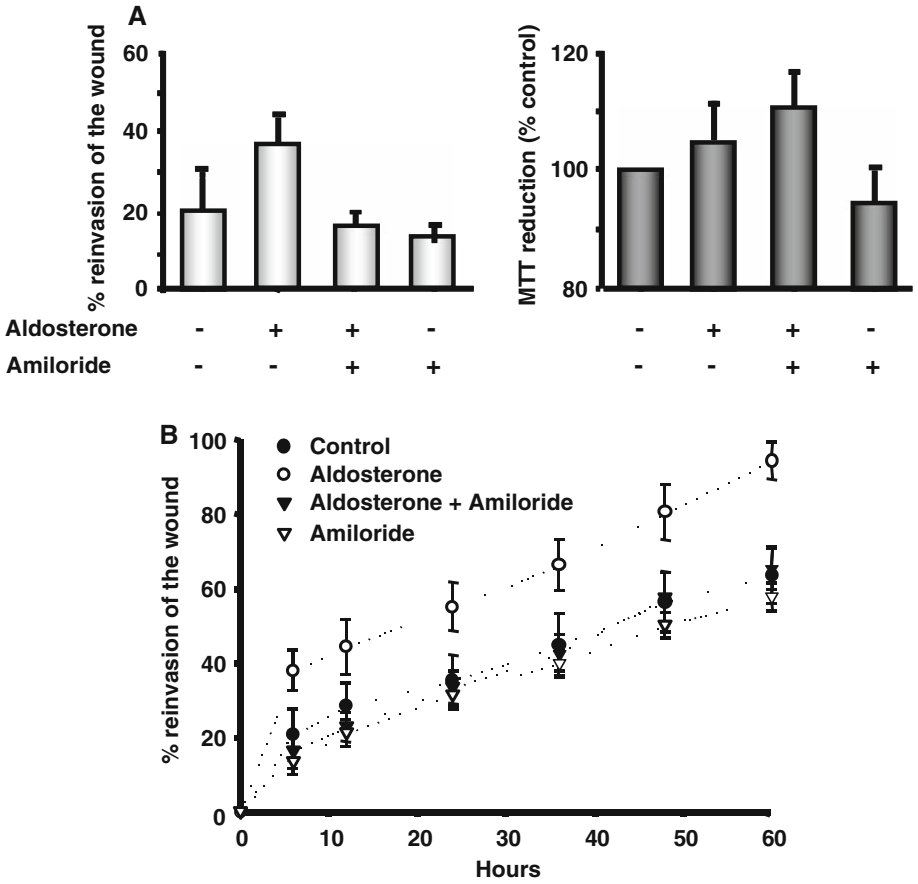

Fig. 2 **a** Cell migration 6 h after wounding. Left Percentage of reinvasion of the wound for the four treatments studied. Aldosterone-treated BeWo cells closed a greater percentage of the wound than the rest of the treatments ($P < 0.05$, $n = 16$). Right MTT cell viability assay for measuring cellular growth. Results are expressed as MTT reduction (compared to control treatment). Reduction takes place only when mitochondrial reductase enzymes are active, and therefore, conversion can be directly related to the number of viable (living) cells. No difference in reduction was observed between the treatments ($n = 12$). **b** Temporal development of the wound-healing assay. Comparison of wound closure in the four treatments studied. Pictures were taken at different times, and wound width was calculated as cells were migrating to close the scratched area. Results are expressed as percentage of reinvasion of the original wound width, at the beginning of the experiment (mean ± SD, $n = 16$). Aldosterone-treated BeWo cells closed a greater percentage of the wound than the rest of the studied treatments ($P < 0.05$)

cells lowered their viability in every treatment, reinforcing the idea that proliferation does not influence wound closure (data not shown).

Antisense Oligonucleotides Against α-ENaC

To further determine if ENaC was participating in the wound-healing effect observed, BeWo cells were treated with antisense or sense oligonucleotides to the AUG-bearing α-ENaC sequence. The experiments were performed as previously described in control conditions, with culture medium only supplemented with aldosterone or in aldosterone-treated BeWo cells plus either antisense or sense α-ENaC oligonucleotides. Figure 3a shows that cells treated with the antisense sequence evidenced a significantly reduced migration compared to the sense treated cells or the cells without oligonucleotide treatment ($P < 0.001, n = 16$; $30.2 \pm 3.7\%$, $17.6 \pm 1.3\%$, $27.5 \pm 1.5\%$, $20.2 \pm 1.5\%$ reinvasion of the wound with aldosterone, aldosterone plus antisense and aldosterone plus sense treatments or control conditions, respectively). In addition, antisense treated cells behaved similar to the cells cultured without aldosterone stimulation. This result suggests that the channel may participate in the wound-healing process observed in aldosterone-treated cells.

To confirm that the oligonucleotide treatment indeed reduced α-ENaC expression in BeWo cells, we obtained protein extracts from these cells to perform Western blot studies. We observed that antisense treatment reduced the subunit expression of the 30-kDa polypeptide compared to the aldosterone-treated cells or the aldosterone plus sense oligonucleotides treated cells (Fig. 3b). This polypeptide corresponds to the α-ENaC N-terminal proteolytic fragment observed previously by our group (del Mónaco et al. 2008b).

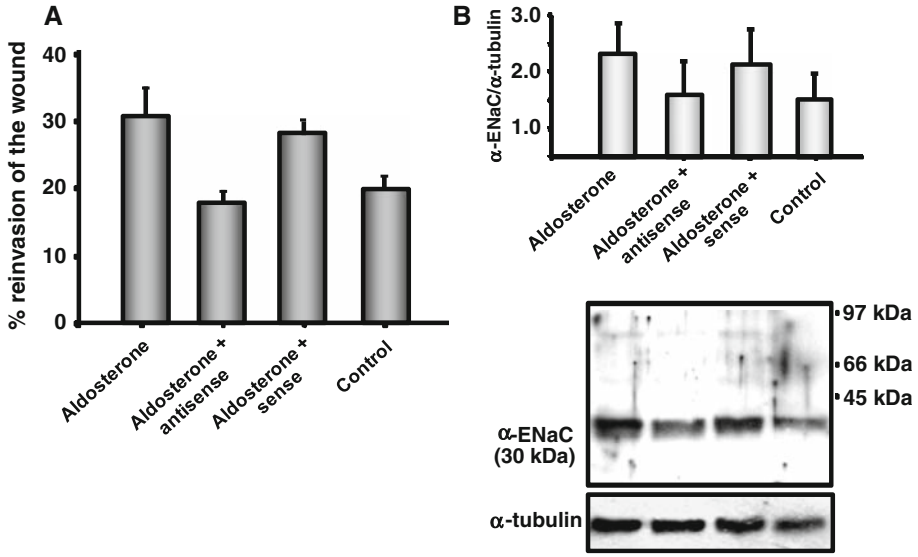

Fig. 3 Antisense oligonucleotides inhibit α-ENaC expression. **a** Wound-healing assay with BeWo cells treated overnight with antisense and sense oligonucleotides, directed against the translation start site of α-ENaC. Antisense treatment produced a reduction in cell migration after injury compared with sense treated cells and nontreated cells ($P < 0.001$, $n = 16$). **b** Expression of the α-ENaC subunit was analyzed by Western blotting of total lysates from BeWo cells after each treatment. Antisense treated cells evidenced reduced α-ENaC expression. The relative level of the protein in each treatment using α-tubulin as an internal control is represented in the upper bar graph ($n = 3$). A representative blot is shown at the bottom

We performed control experiments with normal rabbit IgG to confirm the specificity of the band obtained (data not shown).

Whole-Cell Studies in BeWo Cells Treated with Oligonucleotides Against α-ENaC

To further assess if the oligonucleotide treatment against α-ENaC generated a physiological effect in BeWo cells, we determined current activity by patch clamp in oligonucleotide-treated cells by measuring basal currents in response to depolarizing and hyperpolarizing pulses. We used 8Br-cAMP, a membrane-permeable cAMP analogue, to induce channel exposition to the cell surface (del Mónaco et al. 2008b). Figure 4a shows average current densities (current per unit cell capacitance, pA/pF) vs. voltages from cells cultured with antisense oligonucleotides (left, $n = 3$) and sense oligonucleotides (right, $n = 4$), both supplementing culture medium with aldosterone. Current densities were measured before and after stimulation with 100 μM 8Br-cAMP and after adding 10 μM amiloride to the bath solution (with cAMP). No significant amiloride-sensitive current was observed with the antisense treatment. On the other hand, when cells were cultured with sense oligonucleotides, cAMP activation was observed with an amiloride-sensitive component. Under this treatment, we observed a current increase in every pulse applied after adding cAMP to the bath solution ($P < 0.05$) and a significant decrease after the addition of amiloride ($P < 0.05$). Figure 4b shows the amiloride-sensitive current (I_{amil}) observed in the pulse of −140 mV for both treatments and the significant difference observed between them ($P < 0.05$).

Even though there was α-ENaC protein expression observed by Western blot in the antisense treatments (a lesser amount than that observed in the sense experiments), none of the tested cells showed the amiloride-sensitive current.

ENaC Expression in the Wound

Immunocytochemistry studies showed that the three ENaC subunits were more abundantly expressed in the cells at the leading edge of the wound 3 h after injury (Fig. 5). Fluorescence intensity was assessed using image-processing software, measuring gray-scale intensity in a line perpendicular to the linear wound. The intensity peak of the fluorescence was registered in the pixels between the wound limits (lower plots).

ENaC Expression in Human Placenta

To validate our human placental model, we confirmed expression of the channel in human placenta. RT–PCR analyses of mRNA isolated from placental villi demonstrated the presence of ENaC mRNA. Figure 6a shows the

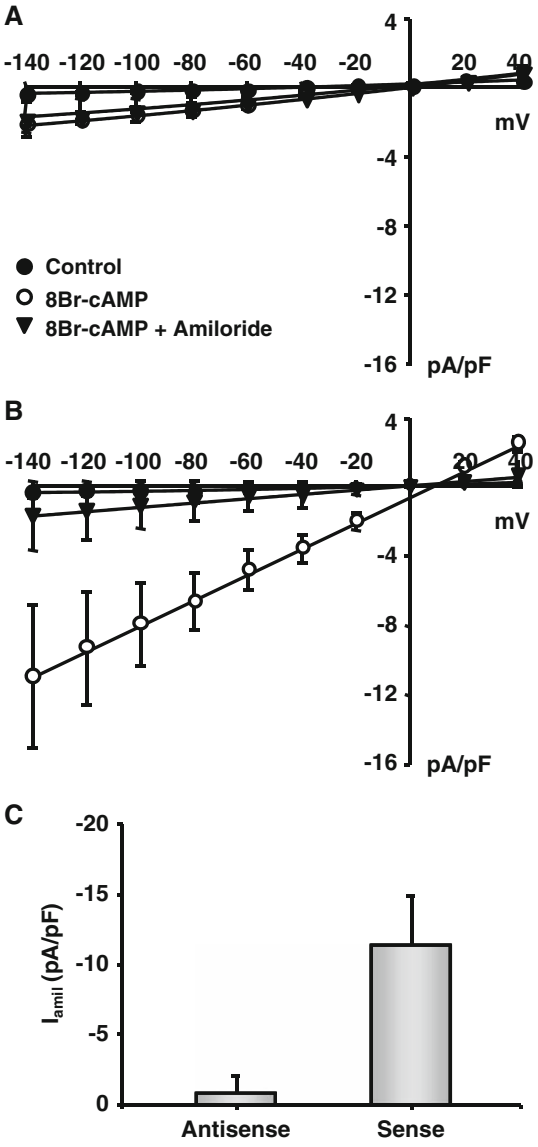

Fig. 4 Whole-cell currents in oligonucleotide-treated BeWo cells. **a** Relationship between current density (current per unit cell capacitance, pA/pF, media ± sd) and the voltages applied. BeWo cells were cultured with aldosterone and antisense oligonucleotides ($n = 3$). **b** Relationship between current density (pA/pF, media ± SD) and the voltage for cells cultured with aldosterone and sense oligonucleotides ($n = 4$). Sense-treated cells showed a current increase in every pulse applied when exposed to cAMP ($P < 0.05$), and that current was blocked afterward with amiloride ($P < 0.05$). Antisense-treated cells showed no current increase. c Amiloride-sensitive current (I_{amil}) (current per unit cell capacitance, pA/pF, media ± sd) for the pulse of −140 mV

amplification products corresponding to the subunits of ENaC, α-ENaC (257 bp), β-ENaC (277 bp) and γ-ENaC (237 bp). Figure 6b shows the sequence of the amplified fragment of α-ENaC. In human placenta this protein has 100% identity with the sequence of α-ENaC obtained from databases (GenBank accession number AAH62613, Swiss-Prot accession number P37088).

We examined by immunohistochemistry if the ENaC subunits may be translated into proteins in human placenta. Figure 7 shows that the channel is present in the polarized syncytium.

Discussion

In this work we tested the effects of aldosterone and amiloride on wound healing and cell migration. When cells were cultured in 1% FBS concentration, the reinvasion of the wound measured 6 h after the injury was about 20% of its initial value and 65% after 60 h. The key finding of this work is that aldosterone enhances cell migration, most likely through its effects upon the ENaC. Expression of the ENaC is not enough to generate this effect because the channel must be transporting ions to induce an accelerated migratory response since amiloride (a pore occlusive blocker) reversed the aldosterone-positive modulation. However, amiloride treatment only inhibited wound healing to control levels. This result suggests that aldosterone-mediated stimulation of ENaC is needed to generate a significant effect and that it is not observed under basal conditions. In a previous work from our laboratory we observed that BeWo cells only presented amiloride-sensitive whole-cell currents when treated with aldosterone (del Mónaco et al. 2008b). We also observed that under basal conditions the cells express only the α-ENaC subunit, instead of the three subunits α-, β- and γ-ENaC, detected in aldosterone-treated cells. This may imply that the heterotrimer αβγ-ENaC is needed to influence wound healing, instead of a homomeric α-ENaC.

Since the Na^+/H^+ exchanger (NHE1) is present in BeWo cells (Silva et al. 1997) and it has been related to cell migration (Schwab et al. 2005), we decided to study antisense oligonucleotides directed to the α-ENaC subunit to isolate ENaC participation in aldosterone-treated cells. Antisense exposed cells covered a lesser surface of the wound, and the ENaC protein showed reduced expression. We also observed that ENaC subunits were expressed more profusely in cells near the wound border, supporting the notion that this protein participates in a postinjury signal. In addition, cells treated with the antisense oligos showed no detectable amiloride-sensitive currents, while the sense treatment showed currents similar to the ones previously observed for aldosterone-stimulated BeWo cells (del Mónaco, et al. 2008b).

Cellular proliferation could mask the contribution of migration to wound healing (Grifoni et al. 2006). To test this, we measured cell proliferation with the MTT assay. In a homogenous sample of cells (like the BeWo cell line), MTT reduction is proportional to the number of metabolically active cells and is used as an indicator of cell

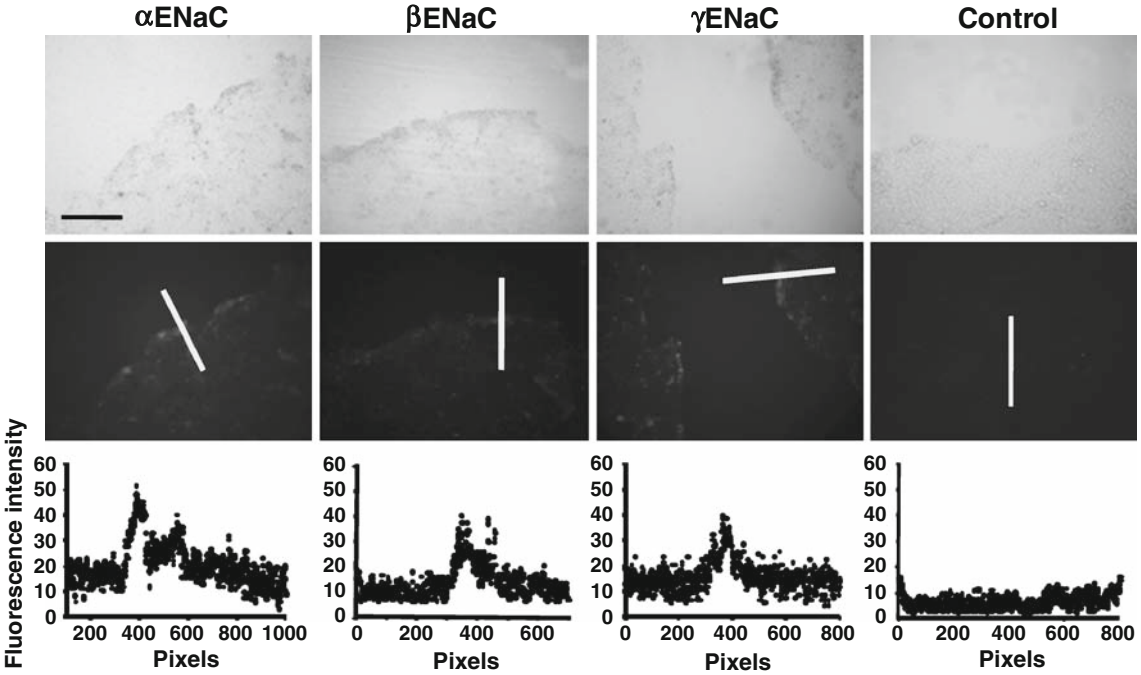

Fig. 5 ENaC expression in the wound. Images of BeWo epithelial sheets cultured with aldosterone 100 nm and wounded by scratching. Monolayers were fixed 3 h after wounding and stained. Each column shows the result using a different ENaC subunit antibody and the control (without primary antibody). Upper image is a phase-contrast image of the wounded monolayer. Black bar = 50 μM. Middle image is ENaC immunofluorescence for the same region studied in the upper image. White bar represents the length plotted for fluorescence intensity, shown in the lower image. Results indicate an increase in subunit fluorescence observed along the wound border

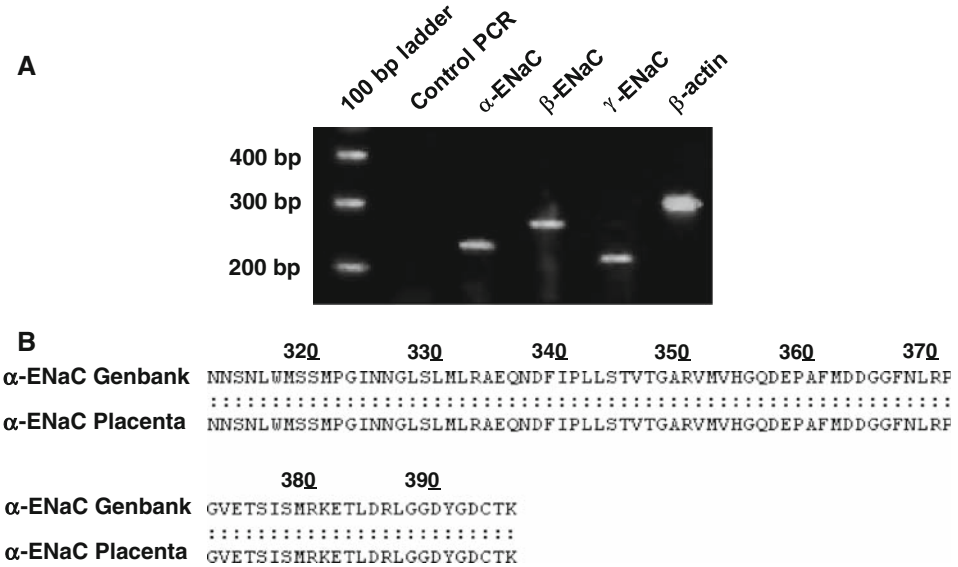

Fig. 6 ENaC expression in human syncytiotrophoblast. **a** Detection of ENaC mRNA: lane 1 molecular weight ladder, lane 2 PCR negative control, lane 3 α-subunit (257 bp), lane 4 *β*-subunit (237 bp), lane 5 *γ*-subunit (237 bp), lane 6 positive control of *β*-actin (289 bp). **b** Sequence analysis of human syncytiotrophoblast cDNA. Amino acid sequence of the α-ENaC subunit fragment cloned from placenta in our laboratory, showing 100% identity with the sequence of the α-ENaC protein obtained from databases (GenBank accession number AAH62613, Swiss-Prot accession number P37088). Numbers correspond to the actual amino acid position in the full-length human α-ENaC protein

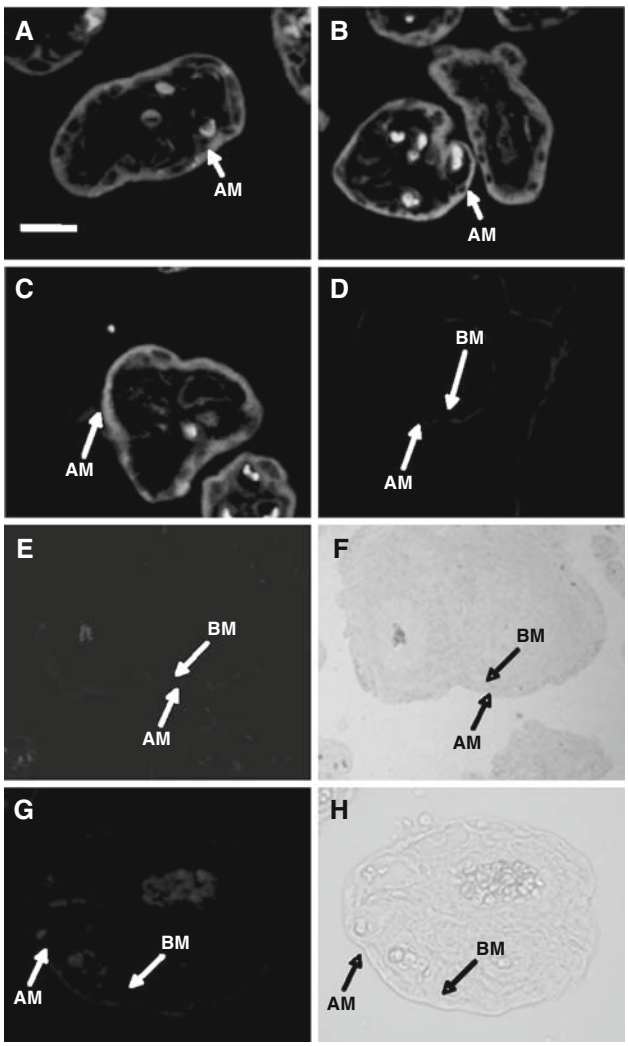

Fig. 7 Immunohistochemistry studies in human syncytiotrophoblast. Localization of ENaC proteins in the syncytiotrophoblast with fluorescence microscopy. Positive staining observed in normal tissues incubated with a polyclonal antibody anti-α-ENaC (**a**), a monoclonal anti-β-ENaC (**b**) and a polyclonal antibody anti-γ-ENaC (**c**). The control for the experiments of β-ENaC was performed without primary antibody but with anti-mouse-FITC (**d**). The controls for the experiments of α- and γ-ENaC were performed incubating the samples without primary antibody but with anti-rabbit-FITC (**e**) or with normal rabbit whole IgG and anti-rabbit-FITC (**g**). Tissue integrity of **e** and **c** was tested (**f** and **h**, respectively). The data are representative of three experiments under each condition. AM: apical membrane; BM: basal membrane. The white bar represents 200 mm

proliferation or viability. Our results show that neither aldosterone nor amiloride increases the proliferation of BeWo cells cultured in 1% FBS concentration, although it has been observed that aldosterone stimulates proliferation of cardiac fibroblasts (Stockhand and Meszaros 2002).

Cell invasion is related to a methylation-dependent repression of adherent junction molecules, as shown in BeWo cells by Rahnama et al. (2006). Aldosterone stimulates a carboxymethylation reaction on the β-subunit of ENaCs, increasing its open probability as an acute stimulatory effect (Rokaw et al. 1998; Becchetti et al. 2000; Le Moëllic et al. 2004; Edinger et al. 2006). This effect did not require de novo expression of the ENaC subunits, so the presence of a membrane receptor to translate the signal was suggested instead (Le Moëllic et al. 2004; Edinger et al. 2006). A generalized modulation of aldosterone in wound healing could be explained partly by this posttranscriptional modification by methyltransferases.

Since BeWo cells are a trophoblast-derived cell line, we decided to confirm the presence of the ENaC in placental tissues. Molecular biological techniques allowed us to detect the channel mRNA and protein expression in the human syncytiotrophoblast. Although the role of ENaC in placenta is still poorly understood, its presence may have consequences for ion and nutrient transport, leading to fetal growth; and the results presented here may be relevant in the preeclampsia condition (Sibai et al. 2005; Myatt 2006). In preeclamptic placentas, impaired arterial remodeling, which normally leads to the formation of maternal lacunae, compromises placental and fetal blood flow (Rahnama et al. 2006; see also Huppertz 2008, for a detailed discussion). This impairment implies that trophoblast cells migrate and invade at a lesser rate. The consequent hypoxia generated may affect the whole placental physiology, as observed in other tissues exposed to hypoxic conditions where sodium and fluid transport was compromised (Jain and Sznajde 2005; Bouvry et al. 2006). Indeed, ENaC expression is altered under low-oxygen environments (Rotin et al. 1994; Planès et al. 2002; Thome et al. 2003), potentiating the effect. It is important to note that aldosterone plasma levels are decreased about 50% in preeclamptic pregnancies compared to normotensive ones (Langer et al. 1998; Shojaati et al. 2004) and downregulated by proinflammatory cytokines (TNF-α, IL-1, etc.) (Natarajan et al. 1989), which are released and elevated in the blood of women with preeclampsia (Bowen et al. 2002 for a review; see also Redman and Sargent 2003).

Given the results presented in this work, we suggest that the actual presence of the heterotrimeric αβγ-ENaC in the syncytiotrophoblast influences cell migration. Our model implies that the channel must be active and that it is sensitive to hormonal stimulation. Under these circumstances, the sodium entering the cells through the ENaC could be an intracellular signal before cells start to migrate. Other authors have implied that ENaC Na^+ transport and the consequent water movement favor the cell swelling required for lamellipodium expansion (Kapoor et al. 2009) as well as the notion that the depolarization generated by ENaC stimulates cytoskeletal reorganization (Chifflet et al. 2005). On the other hand, a growing body of evidence suggests that the ENaC may function as a mechanosensor, interacting with the cytoskeleton and the extracellular

matrix and generating a mechanically gated sodium influx which triggers a secondary signal-transduction pathway (Carattino et al. 2004; Drummond et al. 2004, 2006; Wei et al. 2007). In all these cases, the inhibitory effect of amiloride on BeWo cell migration that we observed can be explained.

Acknowledgement This work was supported by grants from the University of Buenos Aires (MO35) and SECyT (PICT 38181). S. M. d. M. and G. M. have fellowships from the National Council of Research (CONICET) and SECyT, respectively. Y. A., A. D. and B. A. K. are members of CONICET.

References

Alvarez de la Rosa D, Li H, Canessa CM (2002) Effects of aldosterone on biosynthesis, traffic, and functional expression of epithelial sodium channels in A6 cells. J Gen Physiol 119:427–442

Becchetti A, Kemendy AE, Stockand JD, Sariban-Sohraby S, Eaton DC (2000) Methylation increases the open probability of the epithelial sodium channel in A6 epithelia. J Biol Chem 275: 16550–16559

Berdiev BK, Prat AG, Cantiello HF et al (1996) Regulation of epithelial sodium channels by short actin filaments. J Biol Chem 271:17704–17710

Bouvry D, Planés C, Malbert-Colas L et al (2006) Hypoxia-induced cytoskeleton disruption in alveolar epithelial cells. Am J Respir Cell Mol Biol 35:519–527

Bowen JM, Chamley L, Keelan JA, Mitchell MD (2002) Cytokines of the placenta and extra-placental membranes: roles and regulation during human pregnancy and parturition. Placenta 23:257–273

Bubien JK, Watson B, Khan MA et al (2001) Expression and regulation of normal and polymorphic epithelial sodium channel by human lymphocytes. J Biol Chem 276:8557–8566

Butterworth MB, Edinger RS, Frizzell RA, Johnson JP (2009) Regulation of the epithelial sodium channel by membrane trafficking. Am J Physiol 296:F10–F24

Caldwell RA, Boucher RC, Stutts MJ (2004) Serine protease activation of near-silent epithelial Na^+ channels. Am J Physiol 286:C190–C194

Cantiello HF, Stow JL, Prat AG, Ausiello DA (1991) Actin filaments regulate epithelial Na^+ channel activity. Am J Physiol 261: C882–C888

Carattino MD, Sheng S, Kleyman TR (2004) Epithelial Na^+ channels are activated by laminar shear stress. J Biol Chem 279:4120–4126

Chifflet S, Hernández JA, Grasso S (2005) A possible role for membrane depolarization in epithelial wound healing. Am J Physiol 288:C1420–C1430

Copeland SJ, Berdiev BK, Ji HL, Lockhart J, Parker S, Fuller CM, Benos DJ (2001) Regions in the carboxy terminus of alpha-bENaC involved in gating and functional effects of actin. Am J Physiol 281:C231–C240

del Mónaco S, Assef Y, Damiano A, Zotta E, Ibarra C, Kotsias BA (2006) Caracterización del canal epitelial de sodio en sincicio-trofoblasto de placenta humana pre-eclámptica. Medicina (B Aires) 66:31–35

del Mónaco SM, Marino G, Assef Y, Kotsias BA (2008a) Pre-eclampsia, migración cellular y canales iónicos. Medicina (B Aires) 68:405–410

del Mónaco S, Assef Y, Kotsias BA (2008b) Epithelial sodium channel in a human trophoblast cell line (BeWo). J Membr Biol 223:127–139

Diakov A, Bera K, Mokrushina M, Krueger B, Korbmacher C (2008) Cleavage in the γ-subunit of the epithelial sodium channel (ENaC) plays an important role in the proteolytic activation of near-silent channels. J Physiol 586:4587–4608

Drummond HA, Gebremedhin D, Harder DR (2004) Mechanosensor degenerin/epithelial Na^+ channel proteins: components of a vascular mechanosensor. Hypertension 44:643–648

Drummond HA, Furtado MM, Myers S et al (2006) ENaC proteins are required for NGF-induced neurite growth. Am J Physiol 290:C404–C410

Edinger RS, Yospin J, Perry C et al (2006) Regulation of epithelial Na^+ channels (ENaC) by methylation, a novel methyltransferase stimulates ENaC activity. J Biol Chem 281:9110–9117

Forbes K, Desforges M, Garside R, Aplin JD, Westwood M (2009) Methods for siRNA-mediated reduction of mRNA and protein expression in human placental explants, isolated primary cells and cell lines. Placenta 30:124–129

Gambling L, Dunford S, Wilson CA, McArdle HJ, Baines DL (2004) Estrogen and progesterone regulate alpha, beta, and gammaE-NaC subunit mRNA levels in female rat kidney. Kidney Int 65:774–781

Golestaneh N, Klein C, Valamanesh F, Suarez G, Agarwal MK, Mirshahi M (2001) Mineralocorticoid receptor-mediated signaling regulates the ion gated sodium channel in vascular endothelial cells and requires an intact cytoskeleton. Biochem Biophys Res Commun 280:1300–1306

Grifoni SC, Gannon KP, Stec DE, Drummond HA (2006) ENaC proteins contribute to VSMC migration. Am J Physiol 291: H3076–H3086

Harris M, Firsov D, Vuagniaux G, Stutts MJ, Rossier BC (2007) A novel neutrophil elastase inhibitor prevents elastase activation and surface cleavage of the epithelial sodium channel expressed in Xenopus laevis oocytes. J Biol Chem 282:58–64

Hughey RP, Mueller GM, Bruns JB et al (2003) Maturation of the epithelial Na^+ channel involves proteolytic processing of the alpha- and gamma-subunits. J Biol Chem 278:37073–37082

Huppertz B (2008) Placental origins of preeclampsia: challenging the current hypothesis. Hypertension 51:970–975

Jain M, Sznajde JI (2005) Effect of hypoxia on the alveolar epithelium. Proc Am Thorac Soc 2:202–205

Kapoor N, Bartoszewski R, Qadri YJ, et al (2009) Knockdown of ASIC1 and ENaC subunits inhibits glioblastoma whole cell current and cell migration. J Biol Chem. doi:10.1074/jbc.M109.037390

Kellenberger S, Schild L (2002) Epithelial sodium channel/degenerin family of ion channels: a variety of functions for a shared structure. Physiol Rev 82:735–767

Kemendy AE, Kleyman TR, Eaton DC (1992) Aldosterone alters the open probability of amiloride-blockable sodium channels in A6 epithelia. Am J Physiol 263:C825–C837

Langer B, Grima M, Coquard C, Bader AM, Schlaeder G, Imbs JL (1998) Plasma active renin, angiotensin I, and angiotensin II during pregnancy and in preeclampsia. Obstet Gynecol 91: 196–202

Le Moëllic C, Ouvrard-Pascaud A, Capurro C et al (2004) Early nongenomic events in aldosterone action in renal collecting duct cells: PKCalpha activation, mineralocorticoid receptor phosphorylation, and cross-talk with the genomic response. J Am Soc Nephrol 15:1145–1160

Ma HP, Al-Khalili O, Ramosevac S, Saxena S, Liang YY, Warnock DG, Eaton DC (2004) Steroids and exogenous gamma-ENaC subunit modulate cation channels formed by alpha-ENaC in human B lymphocytes. J Biol Chem 279:33206–33212

Malik B, Price SR, Mitch WE, Yue Q, Eaton DC (2006) Regulation of epithelial sodium channels by the ubiquitin-proteasome proteolytic pathway. Am J Physiol 290:F1285–F1294

May A, Puoti A, Gaeggeler HP, Horisberger JD, Rossier BC (1997) Early effect of aldosterone on the rate of synthesis of the epithelial sodium channel alpha subunit in A6 renal cells. J Am Soc Nephrol 8:1813–1822

Mazzochi C, Bubien JK, Smith PR, Benos DJ (2006) The carboxyl terminus of the alpha-subunit of the amiloride-sensitive epithelial sodium channel binds to F-actin. J Biol Chem 281:6528–6538

McEneaney V, Harvey BJ, Thomas W (2008) Aldosterone regulates rapid trafficking of epithelial sodium channel subunits in renal cortical collecting duct cells via protein kinase D activation. Mol Endocrinol 22:881–892

Mills JW, Mandel LJ (1994) Cytoskeletal regulation of membrane transport events. FASEB J 8:1161–1165

Mitchison TJ, Cramer LP (1996) Actin-based cell motility and cell locomotion. Cell 84:371–379

Myatt L (2006) Placental adaptive responses and fetal programming. J Physiol 572:25–30

Natarajan R, Ploszaj S, Horton R, Nadler J (1989) Tumor necrosis factor and interleukin-1 are potent inhibitors of angiotensin-II-induced aldosterone synthesis. Endocrinology 125:3084–3089

Planès C, Blot-Chabaud M, Matthay MA, Couette S, Uchida T, Clerici C (2002) Hypoxia and beta 2-agonists regulate cell surface expression of the epithelial sodium channel in native alveolar epithelial cells. J Biol Chem 277:47318–47324

Rahnama F, Shafiei F, Gluckman PD, Mitchell MD, Lobie PE (2006) Epigenetic regulation of human trophoblastic cell migration and invasion. Endocrinology 147:5275–5283

Reddy MM, Wang XF, Quinton PM (2008) Effect of cytosolic pH on epithelial Na^+ channel in normal and cystic fibrosis sweat ducts. J Membr Biol 225:1–11

Redman CW, Sargent IL (2003) Pre-eclampsia, the placenta and the maternal systemic inflammatory response—a review. Placenta 24 Suppl A:S21–S27

Rokaw MD, Wang JM, Edinger RS et al (1998) Carboxylmethylation of the beta subunit of xENaC regulates channel activity. J Biol Chem 273:28746–28751

Rotin D, Bar-Sagi D, O'Brodovich H et al (1994) An SH3 binding region in the epithelial Na^+ channel (alpha rENaC) mediates its localization at the apical membrane. EMBO J 13:4440–4450

Schwab A, Rossmann H, Klein M et al (2005) Functional role of Na^+-$HCO3^-$ cotransport in migration of transformed renal epithelial cells. J Physiol 568:445–458

Shojaati K, Causevic M, Kadereit B et al (2004) Evidence for compromised aldosterone synthase enzyme activity in pre-eclampsia. Kidney Int 66:2322–2328

Sibai B, Dekker G, Kupferminc M (2005) Pre-eclampsia. Lancet 365:785–799

Silva NL, Wang H, Harris CV, Singh D, Fliegel L (1997) Characterization of the Na^+/H^+ exchanger in human choriocarcinoma (BeWo) cells. Pfluegers Arch 433:792–802

Smith PR, Saccomani G, Joe EH, Angelides KJ, Benos DJ (1991) Amiloride-sensitive sodium channel is linked to the cytoskeleton in renal epithelial cells. Proc Natl Acad Sci USA 88:6971–6975

Snyder PM (2005) Minireview. Regulation of epithelial Na^+ channel trafficking. Endocrinology 146:5079–5085

Sparks RL, Pool TB, Smith NK, Cameron IL (1983) Effects of amiloride on tumor growth and intracellular element content of tumor cells in vivo. Cancer Res 43:73–77

Stockhand JD, Meszaros JG (2002) Aldosterone stimulates proliferation of cardiac fibroblasts by activating Ki-RasA and MAPK1/2 signaling. Am J Physiol 284:H176–H184

Thome UH, Davis IC, Nguyen SV, Shelton BJ, Matalon S (2003) Modulation of sodium transport in fetal alveolar epithelial cells by oxygen and corticosterone. Am J Physiol 284:L376–L385

Verrey F, Fakitsas P, Adam G, Staub O (2008) Early transcriptional control of ENaC (de)ubiquitylation by aldosterone. Kidney Int 73:691–696

Vila-Carriles WH, Kovacs GG, Jovov B et al (2006) Surface expression of ASIC2 inhibits the amiloride-sensitive current and migration of glioma cells. J Biol Chem 281:19220–19232

Wakida N, Kitamura K, Tuyen DG et al (2006) Inhibition of prostasin-induced ENaC activities by PN-1 and regulation of PN-1 expression by TGF-beta1 and aldosterone. Kidney Int 70:1432–1438

Wei SP, Li XQ, Chou CF et al (2007) Membrane tension modulates the effects of apical cholesterol on the renal epithelial sodium channel. J Membr Biol 220:21–31